IOP Publishing Physica Scripta
Phys. Scr. 95 (2020) 035211 (13pp) https://doi.org/10.1088/1402-4896/ab4ba9

Numerical study of transport phenomena in a nanofluid using fractional relaxation times in Buongiorno model

Muhammad Shoaib Anwar

Department of Basic Sciences and Humanities, Narowal Campus, University of Engineering and Technology, Lahore 54890, Pakistan

E-mail: shoaib_tts@uet.edu.pk

Received 21 July 2019, revised 23 September 2019
Accepted for publication 7 October 2019
Published 4 February 2020

Abstract

Convective phenomena in a nanofluid flow under the influence of gravitational and magnetic body forces is analyzed in this communication. Nanofluid is of viscoelastic nature that preserves viscosity as well as elasticity. In order to capture the more realistic behavior of the convective phenomena Caputo fractional derivative and fractional relaxation time are introduced in the Buongiorno nanofluid model. Fractional derivative and relaxation time are used for controlled flow mechanism and to overcome infinite propagation speed for the temperature and concentration. The proposed model will also help to understand the hereditary and memory properties of the viscoelastic nanofluid. In order to more closely analyze the buoyancy forces nonlinear convection is introduced in the mathematical modeling of the flow problem. Finite difference-finite element numerical computations are carried out for the governing nonlinear partial differential equations. Quantities of physical interest are computed and discussed for the fractional model. The proposed fractional model can be used to realistically simulate various flow problems in polymer and chemical industries.

Keywords: finite element method, fractional derivatives, magneto-hydrodynamics, nanoparticles

(Some figures may appear in colour only in the online journal)

1. Introduction

In recent times nanofluids gained interest of industrialists due to their efficient use in the production of lightweight materials and discussed by various researchers in literature [1, 2]. Various studies are performed to observe nanofluids flow through micro [3] and macro [4] channels under different flow configurations and their solutions are noted with small perturbation of flow parameters. Particularly viscoelastic nanofluids are used in electrospinning for the mass-production of nanofibers [5, 6]. Nanoparticles suspension in the base fluid to form nanofluid is only possible if there exist interaction between the base fluid and nanoparticles surface to overcome the differences of density. Nanoparticles effectively influence the properties of base fluid. Thermal conductivity of base fluid increases with these particles suspension. As a result significant enhancement in the coefficient of heat transfer may be seen in the flow domain and can not be tackled by traditional correlations [7]. Hence Buongiorno [8] provide an explanation with his nanofluid model that with heated fluid, viscosity of the fluid decreases results in increase of heat transfer. In this article we have introduced Caputo fractional derivative and the fractional relaxation time in the Buongiorno model to control abrupt increase in heat transfer.

Control of heat transfer along with accurate description of viscoelastic behavior [9] can be tackled simultaneously by the improved form of Buongiorno model with fractional derivatives. In recent years fractional calculus gained importance in fluid mechanics and many other branches of science. Impact of fractional calculus with modern fractional operators is seen in viscoelasticity, control theory and electrochemistry [10, 11]. Also, applications of fractional calculus are increasing due to modern advancements in fractional derivatives that are more mathematically and physically reliable for

example Atangana–Baleanu, Caputo–Fabrizio, and Caputo fractional derivatives [12–15]. Sheikh *et al* [13] discussed the importance of Atangana–Baleanu and Caputo–Fabrizio fractional derivatives in flow problems with the presence of chemical reacting species and also compare these two derivatives in order to analyze the heat transfer. Ali *et al* [14] described the combined effect of magnetic body force and fractional derivative on the blood flow, where blood is behaving like a Casson fluid. Magnetic particles are incorporated in the fluid flow and flow is generated by a pressure gradient. Convective phenomena in a fluid flow via fractional derivative combined with temperature and concentration gradients is analyzed by Sheikh *et al* [15]. Physical systems can better be understand by fractional derivatives because they capture hereditary behavior of diverse substances [16–18]. Simulations of nonlinear models with fractional derivatives can estimate experimental data in a better way than the classical fluid models [19] and help to understand microscopic characteristics of governing physical system [20].

In order to control the flow, Lorentz force plays a vital role within the flow domain particularly in viscoelastic problems such as in MHD generators and nuclear reactors. Influence of magnetic body force can help to resist the flow in boundary layer upto feasible extent. Convection, more precisely nonlinear convection has great influence on flow characteristics because transport phenomena is effected by both buoyancy and gravitational forces. It has widespread applications in nuclear reactors, heat ex-changer and boilers. Zhou and Liang [21] presented DDM scheme for unsteady equations with convection and diffusion effects.

For the complete description of transport phenomena we describe mass, energy and momentum transport using mathematical relations. Precisely differential equations are used to describe these mathematical relations along with constitutive expressions that define fluxes of the conserved quantities [22]. Governing differential equations are solved to study transport of chemical species, heat transfer and fluid flow in geology, engineering sciences, material science, meteorology, environmental sciences and medicines. Transport characteristics of diffusivity, viscosity and conductivity are given by molecular contact and Brownian motion [22]. In literature heat along with mass transfer is extensively discussed by numerous researchers. For instance, Salama *et al* [23] solved flow problem through porous medium using the flux approximations. Here, in this study, viscoelastic second grade fluid model is investigated for transport phenomena with nanoparticles suspension in the base fluid. Flow problems in polymer and fiber handling can be attempted via second grade fluid model such as slurries and polymer suspensions [24]. Up till now, fractional nanofluid flows are not tackled appropriately in literature. Fractional problems are mostly solved via various integral transforms. But it is problematic to solve nonlinear coupled equations by integral transforms. Hence numerical techniques are used for solutions of linear and nonlinear models, for instance see [25, 26] and references there in. In this communication, we considered finite difference and finite element numerical schemes for the solution of current fractional flow domain. Numerical results are plotted for numerous values of physical numbers.

In this article we discussed the flow of fractional second grade nanofluid. For the efficient control of heat and mass transfer within the flow domain Buongiorno model is considered with fractional derivative and relaxation time. Flow is restricted within the domain by magnetic body force. Analysis is carried out with flux conditions at moving boundary. Fluid is flowing over a moving plate with normally applied magnetic field to fluid flow. Thermophoresis and pedesis effects are considered in the present flow regime. Space and time variables are discretized by finite element and finite difference schemes respectively to get stabilized solution of flow problem. Effects of numerous physical flow parameters are examined graphically. In section 2, problem modeling via fractional mathematical equations is discussed. Estimation of flow field by propose scheme is given in the section 3. Simulated behaviors are observed in the section 4. Finally, key finding are stated in the section 5.

2. Problem formulation

First we define the Caputo fractional derivative that will be used in the formulation of governing flow problem. The Caputo time fractional left sided derivative of order α where $\alpha \in \mathbb{C}$ and $\Re e\{\alpha\} > 0$ is given by

$$\partial_t^{\alpha}\psi(t) := \frac{1}{\Gamma(p-\alpha)}\int_0^t (t-\tau)^{p-\alpha-1}\frac{\partial^p}{\partial\tau^p}\psi(\tau)\mathrm{d}\tau, \quad p-1 < \Re e\{\alpha\} < p, \quad p \in \mathbb{N}, \tag{2.1}$$

here $\Gamma(\cdot)$ stands for Euler's Gamma function stated as

$$\Gamma(\beta) := \int_{\mathbb{R}} \xi^{\beta-1}\mathrm{e}^{-\xi}\mathrm{d}\xi, \quad \beta \in \mathbb{C}, \quad \Re\{\beta\} > 0.$$

Now consider magneto-hydrodynamic flow of a nanoliquid between the space of never ending plates with non-integer Caputo time derivative and mixed convection. Small particles are suspended in the base liquid. Enclosure between plates is filled with Darcy medium. Neumann conditions are considered at the lower boundary. Heat flux description is given in figure 1. At the initial time plates and liquid are very still. Additionally at that time fluid and plates are at steady temperature θ_0 and concentration ϕ_0. When time increases i.e. $t > 0$, liquid begins moving by the movement of lower boundary. We accept that flow field is depending upon t and y only. Hence, velocity takes the form

$$\mathbf{U} = u(y, t)\mathbf{e}_{\boldsymbol{x}}. \tag{2.2}$$

Rivlin–Ericksen stress tensors that will be used for the construction of momentum equation are given by

$$\mathbb{T}_1 := \mathbf{U} + (\mathbf{U})^{\mathrm{tr}}, \tag{2.3}$$

$$\mathbb{T}_2 := \partial_t[\mathbb{T}_1] + (\mathbf{U}\cdot\nabla)[\mathbb{T}_1] + (\nabla\mathbf{U})\mathbb{T}_1 + \mathbb{T}_1(\nabla\mathbf{U})^{\mathrm{tr}}. \tag{2.4}$$

Moreover Cauchy stress tensor, for the second grade fluid model is given by

$$\mathbb{T} = -p\mathbb{I} + \mu\mathbb{T}_1 + \beta_1\mathbb{T}_2 + \beta_2\mathbb{T}_1^2, \tag{2.5}$$

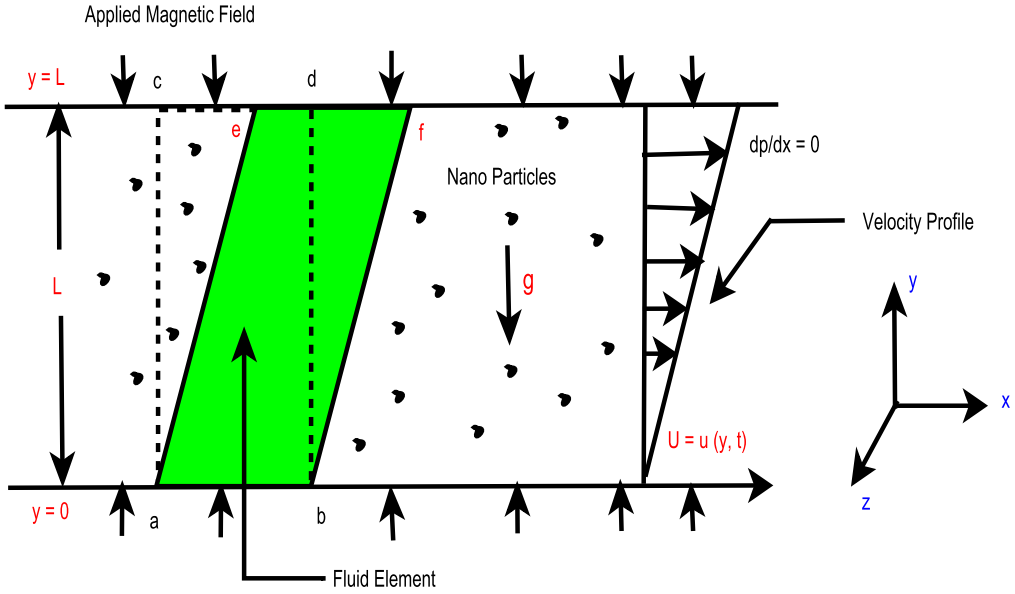

Figure 1. Flow description.

here p denotes fluid hydrostatic pressure and $\mathbb{I}$ stands for identity tensor, $\mu > 0$ represents dynamic viscosity, β_1 and β_2 are material parameters for the second grade model. Moreover, thermodynamic stability requirements for the second grade fluid model are $\beta_1 \geqslant 0$, $\mu \geqslant 0$ and $\beta_1 + \beta_2 = 0$. For the construction of energy equation for nanofluid flow using Caputo fractional derivative, we first consider the energy equation given in Buongiorno paper, for details of used quantities please see [8]

$$\rho_f c_f \left(\frac{\partial}{\partial t} + \nabla \cdot \mathbf{U}\right)\theta = -\nabla \cdot \mathbf{q} + h_p \nabla \cdot \mathbf{J}_p, \tag{2.6}$$

here ρ_f, c_f stand for density and specific heat of the nanofluid, θ denotes the temperature of nanofluid, h_p represents nanoparticles material specific enthalpy, $\mathbf{q}$, $\mathbf{J}_p$ are energy flux and diffusion mass flux respectively.

Since we are dealing with the incompressible fluid so using equation (2.2), we can write equation (2.6) as

$$\rho_f c_f \frac{\partial \theta}{\partial t} = -\nabla \cdot \mathbf{q} + h_p \nabla \cdot \mathbf{J}_p, \tag{2.7}$$

with $\mathbf{q}$ and $\mathbf{J}_p$ are defined as

$$\mathbf{q} = -k\nabla\theta + h_p \mathbf{J}_p, \tag{2.8}$$

and

$$\mathbf{J}_p = -\rho_p D_B \nabla\phi - \rho_p D_\theta \frac{\nabla\theta}{\theta_0}, \tag{2.9}$$

where k, stands for thermal conductivity of the nanofluid, ρ_p denotes the density of nanoparticles, θ_0 represents the reference temperature, ϕ is the concentration, D_θ, D_B are thermal and concentration diffusion coefficients respectively.

Infinite propagation of temperature and concentration can be observed with thermal and concentration flux vectors given in equations (2.8) and (2.9). In order to overcome this situation and following the [27], we can write the equations (2.8) and (2.9) as

$$\left(1 + \frac{\tau_1^\alpha}{\Gamma(1+\alpha)}\frac{\partial^\alpha}{\partial t^\alpha}\right)\mathbf{q} = -k\nabla\theta + h_p\left(1 + \frac{\tau_1^\alpha}{\Gamma(1+\alpha)}\frac{\partial^\alpha}{\partial t^\alpha}\right)\mathbf{J}_p, \tag{2.10}$$

and

$$\left(1 + \frac{\tau_1^\alpha}{\Gamma(1+\alpha)}\frac{\partial^\alpha}{\partial t^\alpha}\right)\mathbf{J}_p = -\rho_p D_B \nabla\phi - \rho_p D_\theta \frac{\nabla\theta}{\theta_0}, \tag{2.11}$$

where τ_1 represents the relaxation time and α stands for Caputo fractional derivative. After applying the operator $\left(1 + \frac{\tau_1^\alpha}{\Gamma(1+\alpha)}\frac{\partial^\alpha}{\partial t^\alpha}\right)$ to equation (2.7), we can write this equation as

$$\rho_f c_f \left(1 + \frac{\tau_1^\alpha}{\Gamma(1+\alpha)}\frac{\partial^\alpha}{\partial t^\alpha}\right)\frac{\partial\theta}{\partial t} = -\left(1 + \frac{\tau_1^\alpha}{\Gamma(1+\alpha)}\frac{\partial^\alpha}{\partial t^\alpha}\right)\nabla \cdot \mathbf{q} + h_p\left(1 + \frac{\tau_1^\alpha}{\Gamma(1+\alpha)}\frac{\partial^\alpha}{\partial t^\alpha}\right)\nabla \cdot \mathbf{J}_p. \tag{2.12}$$

Now using equation (2.10) and after simplification equation (2.12) takes the form

$$\rho_f c_f \left(1 + \frac{\tau_1^\alpha}{\Gamma(1+\alpha)}\frac{\partial^\alpha}{\partial t^\alpha}\right)\frac{\partial\theta}{\partial t} = k\nabla^2\theta - \left(1 + \frac{\tau_1^\alpha}{\Gamma(1+\alpha)}\frac{\partial^\alpha}{\partial t^\alpha}\right)\mathbf{J}_p \cdot \nabla h_p, \tag{2.13}$$

as $\nabla h_p = c_p \nabla\theta$ [8] and using equation (2.9), we can write equation (2.13) as

$$\rho_f c_f\left(1+\frac{\tau_1^\alpha}{\Gamma(1+\alpha)}\frac{\partial^\alpha}{\partial t^\alpha}\right)\frac{\partial\theta}{\partial t} = k\nabla^2\theta + \rho_p c_p\left(1+\frac{\tau_1^\alpha}{\Gamma(1+\alpha)}\frac{\partial^\alpha}{\partial t^\alpha}\right)\left(D_B\nabla\phi\cdot\nabla\theta+\frac{D_\theta}{\theta_0}\nabla\theta\cdot\nabla\theta\right), \tag{2.14}$$

here c_p is specific heat of nanoparticles. Similarly by following the concentration equation given in Buongiorno paper [8], we proceed as

$$\left(\frac{\partial}{\partial t}+\nabla\cdot\mathbf{U}\right)\phi = -\frac{1}{\rho_p}\nabla\cdot\mathbf{J}_p. \tag{2.15}$$

After applying the operator $\left(1+\frac{\tau_1^\alpha}{\Gamma(1+\alpha)}\frac{\partial^\alpha}{\partial t^\alpha}\right)$ to equation (2.15), we can write this equation as

$$\left(1+\frac{\tau_1^\alpha}{\Gamma(1+\alpha)}\frac{\partial^\alpha}{\partial t^\alpha}\right)\left(\frac{\partial}{\partial t}+\nabla\cdot\mathbf{U}\right)\phi = -\frac{1}{\rho_p}\left(1+\frac{\tau_1^\alpha}{\Gamma(1+\alpha)}\frac{\partial^\alpha}{\partial t^\alpha}\right)\nabla\cdot\mathbf{J}_p. \tag{2.16}$$

Now using equations (2.2) and (2.11) and after simplification equation (2.16) takes the form

$$\left(1+\frac{\tau_1^\alpha}{\Gamma(1+\alpha)}\frac{\partial^\alpha}{\partial t^\alpha}\right)\frac{\partial\phi}{\partial t} = D_B\nabla^2\phi+\frac{D_\theta}{\theta_0}\nabla^2\theta. \tag{2.17}$$

In present study governing equations for the incompressible flow under gravitational and magnetic body forces are given by

$$\nabla\cdot\mathbf{U} = 0, \tag{2.18}$$

$$\frac{\partial\mathbf{U}}{\partial t} = \frac{1}{\rho_f}(\nabla\cdot\mathbb{T}+)+\mathbf{b}+g[\beta_3(\theta-\theta_0)+\beta_4(\theta-\theta_0)^2], \tag{2.19}$$

$$\frac{\partial}{\partial t}\left(1+\frac{\tau_1^\alpha}{\Gamma(1+\alpha)}\frac{\partial^\alpha}{\partial t^\alpha}\right)\theta = \alpha_1\frac{\partial^2\theta}{\partial y^2} + \tau_2\left(1+\frac{\tau_1^\alpha}{\Gamma(1+\alpha)}\frac{\partial^\alpha}{\partial t^\alpha}\right)\left(D_B\frac{\partial\theta}{\partial y}\frac{\partial\phi}{\partial y}+\frac{D_\theta}{\theta_0}\left(\frac{\partial\theta}{\partial y}\right)^2\right), \tag{2.20}$$

$$\frac{\partial}{\partial t}\left(1+\frac{\tau_1^\alpha}{\Gamma(1+\alpha)}\frac{\partial^\alpha}{\partial t^\alpha}\right)\phi = D_B\frac{\partial^2\phi}{\partial y^2}+\frac{D_\theta}{\theta_0}\frac{\partial^2\theta}{\partial y^2}, \tag{2.21}$$

where $\alpha_1 = \frac{k}{(\rho c)_f}$ denotes thermal diffusivity, g stands for gravitational acceleration, $\tau_2 = \frac{(\rho c)_p}{(\rho c)_f}$ denotes heat capacities ratio, β_3 and β_4 are coefficients of thermal expansion and $\mathbf{b}$ stands for magnetic body force.

We assume that there is no pressure gradient.

2.1. Flow equations

The flow equations with associated conditions are given in this segment. Equation (2.18) is identically, satisfied by velocity $\mathbf{U}$ defined in (2.2). After simplification governing equations reduces to

$$\frac{\partial u}{\partial t} = \left(\nu+\frac{\beta_1}{\rho_f}\frac{\partial}{\partial t}\right)\left[\frac{\partial^2 u}{\partial y^2}\right] - \frac{\sigma B_0^2}{\rho_f}u + g[\beta_3(\theta-\theta_0)+\beta_4(\theta-\theta_0)^2], \tag{2.22}$$

$$\frac{\partial}{\partial t}\left(1+\frac{\tau_1^\alpha}{\Gamma(1+\alpha)}\frac{\partial^\alpha}{\partial t^\alpha}\right)\theta = \alpha_1\frac{\partial^2\theta}{\partial y^2} + \tau_2\left(1+\frac{\tau_1^\alpha}{\Gamma(1+\alpha)}\frac{\partial^\alpha}{\partial t^\alpha}\right)\left(D_B\frac{\partial\theta}{\partial y}\frac{\partial\phi}{\partial y}+\frac{D_\theta}{\theta_0}\left(\frac{\partial\theta}{\partial y}\right)^2\right), \tag{2.23}$$

$$\frac{\partial}{\partial t}\left(1+\frac{\tau_1^\alpha}{\Gamma(1+\alpha)}\frac{\partial^\alpha}{\partial t^\alpha}\right)\phi = D_B\frac{\partial^2\phi}{\partial y^2}+\frac{D_\theta}{\theta_0}\frac{\partial^2\theta}{\partial y^2}, \qquad 0<y<L, \quad t>0. \tag{2.24}$$

In the above expressions σ denotes electrical conductivity, ν is the kinematic viscosity and B_0 is external magnetic field.

2.1.1. Flow conditions. Conditions on thermal and concentration gradients are incorporated at lower boundary. Initially, complete flow domain is very still with temperature θ_0 and concentration ϕ_0. Conditions in this case are defined as

$$u(0,t) = A\frac{\nu^2}{L^4}t^2, \qquad u(L,t) = 0, \tag{2.25}$$

$$-k\left(\frac{\partial\theta}{\partial y}\right)_{y=0} = \frac{q_\theta\nu^2}{L^4}t^2 \quad \text{and} \quad \theta(L,t) = \theta_0\left(1+\frac{\nu^2}{L^4}t^2\right), \tag{2.26}$$

$$-D_B\left(\frac{\partial\phi}{\partial y}\right)_{y=0} = \frac{q_\phi\nu^2}{L^4}t^2 \quad \text{and} \quad \phi(L,t) = \phi_0\left(1+\frac{\nu^2}{L^4}t^2\right), \tag{2.27}$$

$$u(y,0)=0, \quad \theta(y,0)=\theta_0, \quad \phi(y,0)=\phi_0 \quad \text{and} \quad \frac{\partial\theta}{\partial t}(y,0) = 0 = \frac{\partial\phi}{\partial t}(y,0). \tag{2.28}$$

Here A is dimensional constant, ϕ_0 is the reference concentration, q_θ, q_ϕ stand for constant heat and concentration fluxes. Complete flow problem is specified by (2.22)–(2.28).

2.1.2. Skin friction coefficient. Relative measure of friction among solid boundaries and fluid is given by friction

coefficient. Here friction coefficients are calculated as

$$\mathcal{C}_f := \frac{2\tau_w}{\rho A^2}, \tag{2.29}$$

where wall shear stress is

$$\tau_w = \left[\left(\mu + \beta_1 \frac{\partial}{\partial t}\right)\frac{\partial u}{\partial y}\right]_{y=0,L}. \tag{2.30}$$

2.1.3. Nusselt numbers. Heat fluxes at the surrounding boundaries are calculated by Nusselt numbers. Nusselt numbers for the governing flow field are defined as

$$Nu_1 = \frac{-L\left(\frac{\partial \theta}{\partial y}\right)_{y=L}}{\theta_{s_1} - \theta_0}, \tag{2.31}$$

where θ_{s_1} is the boundary temperature at $y = L$. At $y = 0$ Nusselt number is defined as

$$Nu_2 = \frac{-L\left(\frac{\partial \theta}{\partial y}\right)_{y=0}}{\theta_{s_2} - \theta_0}, \tag{2.32}$$

here θ_{s_2} is the boundary temperature at $y = 0$.

2.1.4. Sherwood numbers. Mass fluxes at the surrounding boundaries are calculated by Sherwood numbers. Sherwood numbers for the governing flow field are defined as

$$Sh_1 = \frac{-L\left(\frac{\partial \phi}{\partial y}\right)_{y=L}}{\phi_{s_1} - \phi_0}, \tag{2.33}$$

where ϕ_{s_1} denotes concentration at upper boundary. Also, at $y = 0$ we define the Sherwood number as

$$Sh_2 = \frac{-L\left(\frac{\partial \phi}{\partial y}\right)_{y=0}}{\phi_{s_2} - \phi_0}, \tag{2.34}$$

here ϕ_{s_2} is the concentration at the boundary $y = 0$.

2.1.5. Non-dimensionalization of mathematical problem. Consider following dimensionless variables to make the problem (2.22)–(2.28) non-dimensional as

$$\hat{y} := \frac{y}{L}, \quad \hat{t} := \frac{\nu}{L^2}t \quad \hat{u} := \frac{u}{A}, \quad \hat{\theta} := \frac{\theta - \theta_0}{\theta_0} \quad \hat{\phi} := \frac{\phi - \phi_0}{\phi_0}. \tag{2.35}$$

With (2.35), after using dimensionless variables with out hats the IBVP (2.22)–(2.28) takes form

$$\begin{aligned}
&\frac{\partial u}{\partial t} = \left(1 + \gamma\frac{\partial}{\partial t}\right)\left[\frac{\partial^2 u}{\partial y^2}\right] - Hau + (\lambda + \lambda_1\theta)\theta,\\
&Pr\frac{\partial}{\partial t}\left(1 + \delta_2\frac{\partial^\alpha}{\partial t^\alpha}\right)\theta\\
&= \frac{\partial^2\theta}{\partial y^2} + Pr\left(1 + \delta_2\frac{\partial^\alpha}{\partial t^\alpha}\right)\left(Nb\frac{\partial\theta}{\partial y}\frac{\partial\phi}{\partial y} + Nt\left(\frac{\partial\theta}{\partial y}\right)^2\right),\\
&Sc\frac{\partial}{\partial t}\left(1 + \delta_2\frac{\partial^\alpha}{\partial t^\alpha}\right)\phi\\
&= \frac{\partial^2\phi}{\partial y^2} + \left(\frac{Nt}{Nb}\right)\frac{\partial^2\theta}{\partial y^2}, \quad 0 < y < 1, \quad t > 0,
\end{aligned} \tag{2.36}$$

together with following flow conditions

$$\begin{cases}
u(0,t) = t^2, \quad u(1,t) = 0, \quad \left(\frac{\partial\theta}{\partial y}\right)_{y=0} = -\delta t^2, \quad \left(\frac{\partial\phi}{\partial y}\right)_{y=0} = -\delta_1 t^2, \quad \theta(1,t) = t^2 = \phi(1,t),\\
u(y,0) = 0, \quad \theta(y,0) = 0 = \frac{\partial\theta}{\partial t}(y,0) \quad \text{and} \quad \phi(y,0) = 0 = \frac{\partial\phi}{\partial t}(y,0).
\end{cases} \tag{2.37}$$

Here γ denotes the viscoelastic parameter, Ha is magnetic parameter, λ and λ_1 stand for convection parameters, Nb denotes pedesis parameter, Nt is the thermophoresis parameter, δ is heat flux parameter, δ_1 stands for mass flux parameter, δ_2 denotes the relaxation time parameter, Sc is Schmidt number and Pr stands for Prandtl number. Stated dimensionless quantities are defined as

$$\begin{aligned}
&\gamma := \frac{\beta_1}{\rho L^2}, \quad Ha := \frac{\sigma B_0^2 L^2}{\mu}, \quad Pr := \frac{\nu}{\alpha_3},\\
&Sc := \frac{\nu}{D_B}, \quad Nt := \frac{\tau_2 D_\theta}{\nu}, \quad \lambda := \frac{gL^2\beta_3\theta_0}{A\nu},\\
&\lambda_1 := \frac{gL^2\beta_4\theta_0^2}{A\nu}, \quad Nb := \frac{\tau_2\phi_0 D_B}{\nu}, \quad \delta := \frac{q_\theta L}{\theta_0 k},\\
&\delta_1 := \frac{q_\phi L}{\phi_0 D_B}, \quad \delta_2 := \frac{\tau_1^\alpha \nu^\alpha}{\Gamma(1+\alpha)L^{2\alpha}}.
\end{aligned} \tag{2.38}$$

Also non-dimensional friction coefficients, Nussselt and Sherwood numbers are defined by

$$\frac{ReC_f}{2} = \left[\left(1 + \gamma\frac{\partial}{\partial t}\right)\frac{\partial u}{\partial y}\right]_{y=0,1}, \tag{2.39}$$

$$\frac{Nu_1}{Re} = -\left(\frac{\partial\theta}{\partial y}\right)_{y=1} \quad \text{and} \quad \frac{Nu_2}{Re^2} = \delta t^2, \tag{2.40}$$

$$\frac{Sh_1}{Re} = -\left(\frac{\partial \phi}{\partial y}\right)_{y=1} \quad \text{and} \quad \frac{Sh_2}{Re^2} = \delta_1 t^2, \tag{2.41}$$

where $Re = \frac{AL}{\nu}$ represents Reynold's number.

3. Discretization scheme

Discretization of problem (2.36)–(2.37) will be discussed in this section. Non-integer derivative is discretized by finite difference scheme as given by [10, 26] while space variable discretization is carried out by finite element scheme proposed in [10]. The well posedness of problem under consideration, can be verified in suitable functional spaces [26]. In short, we consider no ill-posedness in the problem.

For discretizations of model (2.36)–(2.37), we must introduce proper functional spaces.

We denote the square integrable space $\mathcal{L}^2(\Omega)$ of functions defined on $\Omega = (0, 1)$ with $\mathcal{L}^2-$ norm and inner product. Also, $\mathcal{H}^p(\Omega)$ represents Sobolev space, $p > 0$, $\mathcal{H}_0^p(\Omega)$ is taken as closure of $\mathcal{C}_0^\infty(\overline{\Omega})$ in $\mathcal{H}^p(\Omega)$ and $\mathcal{C}_0^\infty(\overline{\Omega})$ denotes classical infinite continuously differentiable functions, with proper compact support in Ω [28]. Also we consider space

$$\mathcal{H}_1^p(\Omega) = \{\mathbf{u} \in \mathcal{H}^p(\Omega) |\ \ \mathbf{u}|_{y=1} = 0\},$$

with $\mathbb{L}^2(\Omega) = \mathcal{L}^2(\Omega) \times \mathcal{L}^2(\Omega) \times \mathcal{L}^2(\Omega)$ and $\mathbb{H}(\Omega) = \mathcal{H}_0^p(\Omega) \times \mathcal{H}_1^p(\Omega) \times \mathcal{H}_1^p(\Omega)$.

Let $\mathcal{L}^2(0, T; \mathcal{V}(\Omega))$: $[0, t_f] \to \mathcal{V}$ equipped with

$$(u, v)_{\mathcal{L}^2(0,t_f;\mathcal{V}(\Omega))} := \int_0^{t_f} (u, v)_{\mathcal{V}(\Omega)} \mathrm{d}t \quad \text{and}$$

$$\|u\|_{\mathcal{L}^2(0,T;\mathcal{V}(\Omega))} := \left(\int_0^{t_f} \|u\|^2_{\mathcal{V}(\Omega)} \,\mathrm{d}t\right)^{1/2}.$$

Furthermore, $\mathcal{C}^0([0, t_f]; \mathcal{V}(\Omega))$ is the space of continuous functions u: $[0, t_f] \to \mathcal{V}$ with

$$\|u\|_{\mathcal{C}^0([0,t_f];\mathcal{V}(\Omega))} := \max_{t\in[0,t_f]} \|u\|_{\mathcal{V}}.$$

Analogously, for $k \in \mathbb{N}$,

$$\mathcal{C}^k([0, t_f]; \mathcal{V}(\Omega)) := \{u \in \mathcal{C}^0([0, t_f]; \mathcal{V}(\Omega)) |\ \partial_t^j u \in \mathcal{C}^0([0, T]; \mathcal{V}(\Omega)), \forall j \leqslant k: j \in \mathbb{N}\},$$

and

$$\|u\|_{\mathcal{C}^k([0,t_f];\mathcal{V}(\Omega))} := \max_{j=0}^{k} (\|\partial_t^j u\|_{\mathcal{C}^0([0,t_f];\mathcal{V}(\Omega))})$$

and also we denote by $\mathbb{C}^k([0, t_f]; \mathbb{V}(\Omega)) = [\mathcal{C}^k([0, t_f]; \mathcal{V}(\Omega))]^3$.

3.1. Finite difference estimations

Discretization of time variable in (2.36)–(2.37) is carried out by finite difference algorithm. Time interval $[0, t_f]$ is divided by fixing time step $\tau := \frac{t_f}{m}$ such as $t_k := k\tau$, here $k = 0, 1, 2, \cdots, m$. Approximation of time derivative at fixed time t_k, $0 < k < m$

$$\frac{\partial u}{\partial t}(y, t_k) \simeq \frac{u(y, t_{k+1}) - u(y, t_k)}{\tau}, \quad t_k \leqslant s \leqslant t_{k+1}, \tag{3.1}$$

here for $k = 0$,

$$\frac{\partial u}{\partial t}(y, t_0) \simeq \frac{u(y, t_1) - u(y, t_0)}{\tau}.$$

Initial conditions (2.37) give

$$u(y, t_1) \simeq 0 \quad \text{and} \quad u(y, t_0) \simeq 0. \tag{3.2}$$

The non-integer time derivatives ∂_t^α $(0 < \alpha < 1)$ for all $0 \leqslant k < m$ can be estimated using Caputo derivative [26]

$$\partial_t^\alpha \psi(t) := \frac{1}{\Gamma(p - \alpha)} \int_0^t (t - \tau)^{p-\alpha-1} \frac{\partial^p}{\partial \tau^p} \psi(\tau) \mathrm{d}\tau,$$
$$p - 1 < \Re e\{\alpha\} < p, \quad p \in \mathbb{N}, \tag{3.3}$$

with Gamma function $\Gamma(\cdot)$ given by

$$\Gamma(\beta) := \int_{\mathbb{R}} \xi^{\beta-1} \mathrm{e}^{-\xi} \mathrm{d}\xi, \quad \beta \in \mathbb{C}, \quad \Re\{\beta\} > 0.$$

Also, we specify following operators

$$\mathcal{L}_t^\alpha[\theta(\cdot)](t) := \left(\frac{\partial}{\partial t} + \delta_2 \frac{\partial^{(\alpha+1)}}{\partial t^{(\alpha+1)}}\right)[\theta(t)],$$
$$\mathcal{Q}_t^\alpha[\theta(\cdot)](t) := \left(1 + \delta_2 \frac{\partial^\alpha}{\partial t^\alpha}\right)[\theta(t)].$$

Finite difference estimations of the operators $\mathcal{L}_t^\alpha[\theta]$ and $\mathcal{Q}_t^\alpha[\theta]$ can be considered as, please see [20]

$$\mathcal{L}_t^\alpha[\theta](t_{k+1}) = \left(\frac{\partial}{\partial t} + \delta_2 \frac{\partial^{\alpha+1}}{\partial t^{\alpha+1}}\right)[\theta](t_{k+1}),$$
$$\simeq \frac{\theta(t_{k+1}) - \theta(t_k)}{\tau} + C_\alpha[\theta(t_{k+1}) - 2\theta(t_k) + \theta(t_{k-1})]$$
$$+ C_\alpha(\psi_k^\alpha[\theta] - \psi_{k-1}^\alpha[\theta]) \tag{3.4}$$

and

$$\mathcal{Q}_t^\alpha[\theta](t_{k+1}) = \left(1 + \delta_2 \frac{\partial^\alpha}{\partial t^\alpha}\right)[\theta](t_{k+1}),$$
$$\simeq \theta(t_{k+1}) + \delta_2 C_\alpha[\theta(t_{k+1}) - \theta(t_k)] + \delta_2 C_\alpha \psi_k^\alpha[\theta] \tag{3.5}$$

with $c_\alpha = \tau^{-\alpha}/\Gamma(2 - \alpha)$ and where $b_s^\alpha := (s + 1)^{1-\alpha} - (s)^{1-\alpha}$, for $0 \leqslant s \leqslant m$, with

$$\psi_k^\alpha[\theta] := \sum_{s=1}^{k} b_s^\alpha[\theta(y, t_{k+1-s}) - \theta(y, t_{k-s})] \quad \text{with}$$
$$\psi_0^\alpha[\theta] := 0. \tag{3.6}$$

3.2. Finite element discretization

The section describes discretization of spatial variable with finite element scheme. For the discretize of spatial variables define the partition of the domain $\Omega = [0, 1]$ into

n sub-domains $\Omega_i = (y_i, y_{i+1})$ for $i = 1, 2, \ldots, n$, satisfying

$$\overline{\Omega} = \bigcup_{i=1}^{n} \overline{\Omega}_i \quad \text{and} \quad \Omega_i \bigcap \Omega_j = \varnothing, \quad \forall\, i \neq j.$$

The elements Ω_i length h is assumed fixed, i.e. $h \coloneqq \frac{2}{n} \coloneqq y_{i+1} - y_i$. Define a finite dimensional subspace $\{\mathcal{V}_0^h(\Omega)\}_{h>0}$ of $\mathcal{H}_0^1(\Omega)$ and $\{\mathcal{V}_1^h(\Omega)\}_{h>0}$ of $\mathcal{H}_1^1(\Omega)$ by

$$\mathcal{V}_0^h(\Omega) \coloneqq \{\phi \in \mathcal{H}_0^1(\Omega) \mid \quad \phi_{|_{\Omega_i}} \in P_r(\Omega_i), \forall\, i \quad = \quad 1, 2,\cdots,n\}, \tag{3.7}$$

$$\mathcal{V}_1^h(\Omega) \coloneqq \{\phi \in \mathcal{H}_1^1(\Omega) \mid \quad \phi_{|_{\Omega_i}} \in P_r(\Omega_i), \forall\, i \quad = \quad 1, 2,\cdots,n\}, \tag{3.8}$$

where $P_r(\Omega_i)$ is Lagrange polynomials space with degree less than or equal to r over the element Ω_i for all $i = 1, 2,\cdots, n$. Also note that $\mathbb{V}^h(\Omega) = \mathcal{V}_0^h(\Omega) \times \mathcal{V}_1^h(\Omega) \times \mathcal{V}_1^h(\Omega)$.

The weak form of the model problem (2.36)–(2.37) can then be obtained by

Weak Form. Find $(u, \theta, \phi) \in \mathbb{C}^1([0, T]; \mathbb{H}(\Omega))$ such that

$$\begin{cases} \frac{\partial}{\partial t}(u, v) + \left(1 + \gamma\frac{\partial}{\partial t}\right)\langle u, v\rangle + Ha(u, v) - ((\lambda + \lambda_1\theta)\theta, v) = 0, \\ Pr\mathcal{L}_t^\alpha(\theta, \zeta) + \langle\theta, \zeta\rangle - Pr\mathcal{Q}_t^\alpha(\theta, \zeta)\left(Nb\left(\frac{\partial\theta}{\partial y}\frac{\partial\phi}{\partial y}, \zeta\right) + Nt\left(\left(\frac{\partial\theta}{\partial y}\right)^2, \zeta\right)\right) = (-\delta t, \zeta(0)), \\ Sc\mathcal{L}_t^\alpha(\phi, \psi) + \langle\phi, \psi\rangle + \left(\frac{Nt}{Nb}\right)\langle\theta, \psi\rangle = (-\delta t - \delta_1 t, \psi(0)), \\ u(y, 0) = , \theta(y, 0) = 0 = \frac{\partial\theta}{\partial t}(y, 0), \text{ and } \phi(y, 0) = 0 = \frac{\partial\phi}{\partial t}(y, 0) \end{cases}, \tag{3.9}$$

for all $(v, \zeta, \psi) \in \mathbb{H}(\Omega)$. □

Weak form (3.9) can be used to incorporate discrete weak form at specific time $t = t_k$, $0 < k < m$

$$\begin{cases} \text{Find } (u_h(\cdot,t_{k+1}), \theta(\cdot,t_{k+1}), \phi(\cdot,t_{k+1})) \in \mathbb{V}^h(\Omega) \text{ s.t. } \forall (v, \zeta, \psi) \in \mathbb{V}^h(\Omega) \\ \frac{\partial}{\partial t}(u_h(y, t_{k+1}), v) + \left(1 + \gamma\frac{\partial}{\partial t}\right)\langle u_h(y, t_{k+1}), v\rangle + Ha(u_h(y, t_{k+1}), v) \\ \qquad -((\lambda + \lambda_1\theta_h(y, t_{k+1}))\theta_h(y, t_{k+1}), v) = 0, \\ Pr\mathcal{L}_t^\alpha(\theta_h(y, t_{k+1}), \zeta) + \langle\theta_h(y, t_{k+1}), \zeta\rangle - PrNb\mathcal{Q}_t^\alpha\left(\frac{\partial\theta_h(y,t_{k+1})}{\partial y}\frac{\partial\phi_h(y,t_{k+1})}{\partial y}, \zeta\right) \\ \qquad -PrNt\mathcal{Q}_t^\alpha\left(\left(\frac{\partial\theta_h(y,t_{k+1})}{\partial y}\right)^2, \zeta\right) = (-\delta t, \zeta(0)), \\ Sc\mathcal{L}_t^\alpha(\phi_h(y, t_{k+1}), \psi) + \langle\phi_h(y, t_{k+1}), \psi\rangle + \frac{Nt}{Nb}\langle\theta_h(y, t_{k+1}), \psi\rangle = (-\delta t - \delta_1 t, \psi(0)), \\ u_h^0(y) = 0, \ \theta_h^0(y) = 0 = \theta_h^1(y), \ \phi_h^0(y) = 0 = \phi_h^1(y) \end{cases}, \tag{3.10}$$

where $u_h^0(\cdot) = u_h(\cdot, t_0)$, $\theta_h^1(\cdot) = \theta_h(\cdot, t_1)$, $\phi_h^1(\cdot) = \phi_h(\cdot, t_1)$, $\theta_h^0(\cdot) = \theta(\cdot, t_0)$ and $\phi_h^0(\cdot) = \phi(\cdot, t_0)$. The approximate solution (u_h, θ_h, ϕ_h) to (3.10) is defined as

$$u_h(y, t_{k+1}) = \sum_{p=1}^{N_h} u_p(t_{k+1}) W_{0h}^p(y), \qquad y \in \overline{\Omega}, \tag{3.11}$$

$$\theta_h(y, t_{k+1}) = \sum_{l=1}^{N_h} \theta_l(t_{k+1}) W_{1h}^l(y), \qquad y \in \overline{\Omega}, \tag{3.12}$$

$$\phi_h(y, t_{k+1}) = \sum_{l=1}^{N_h} \phi_l(t_{k+1}) W_{1h}^l(y), \qquad y \in \overline{\Omega}, \tag{3.13}$$

where $\mathbf{W}_{0h} = \{W_{0h}^p |\, p = 1, 2,\cdots,N_{0h}\}$ forms a basis of $\mathcal{V}_0^h(\Omega)$ with $N_{0h} \coloneqq \dim(\mathcal{V}_0^h)$ and $\mathbf{W}_{1h} = \{W_{1h}^l |\, l = 1, 2,\cdots,N_{1h}\}$ forms a basis of $\mathcal{V}_1^h(\Omega)$ with $N_{1h} \coloneqq \dim(\mathcal{V}_1^h)$ and the parameters (u_p, θ_l, ϕ_l) are to be determined. Therefore, by choosing v as W_{0h}^q for different values of q such that $q = 1, 2,\cdots,N_{0h}$, ζ and ψ as W_{1h}^m for different values of m such that $m = 1, 2,\cdots,N_{1h}$, consequently we obtain the following system of nonlinear algebraic equations

$$\begin{cases} \mathbb{A}_0^h \frac{\mathrm{d}}{\mathrm{d}t}[\mathbf{U}_h] + \tau \mathbb{B}_0^h \left(1 + \gamma \frac{\mathrm{d}}{\mathrm{d}t}\right)[\mathbf{U}_h] + \tau Ha \mathbb{M}_0^h \mathbf{U}_h + \tau \lambda \mathbb{M}_0^h \mathbf{\Theta}_h + \tau \lambda_1 \Theta_h(t_k) \mathbb{M}_0^h \mathbf{\Theta}_h = \mathbf{0}, \\ Pr \mathbb{A}_1^h \mathcal{L}_{k+1}^{\alpha}[\mathbf{\Theta}_h] + \tau \mathbb{B}_1^h \mathbf{\Theta}_h - \tau PrNb \Phi_h(t_k) \mathcal{C}_1^h \mathcal{Q}_{k+1}^{\alpha}[\mathbf{\Theta}_h] - \tau PrNt \theta_h(t_k) \mathcal{C}_1^h \mathcal{Q}_{k+1}^{\alpha}[\mathbf{\Theta}_h] = -\delta t \mathbf{I}, \\ Sc \mathbb{A}_1^h \mathcal{L}_{k+1}^{\alpha}[\mathbf{\Phi}_h] + \tau \mathbb{B}_1^h \mathbf{\Phi}_h + \tau \frac{Nt}{Nb} \mathbb{B}_1^h \mathbf{\Theta}_h = (-\delta t - \delta_1 t)\mathbf{I}, \\ \mathbf{U}_h^0 = \mathbf{0}, \ \mathbf{\Theta}_h^0 = \mathbf{0} = \mathbf{\Theta}_h^1, \ \mathbf{\Phi}_h^0 = \mathbf{0} = \mathbf{\Phi}_h^1, \end{cases} \tag{3.14}$$

where for all $p, q = 1, 2, \cdots, N_{0h}$ and $l, m = 1, 2, \cdots, N_{1h}$.

$$(\mathbf{U}_h)_p := u_p, \quad (\mathbf{\Theta}_h)_l := \theta_l, \quad (\mathbf{\Phi}_h)_l := \phi_l,$$

$$(\mathbb{A}_0^h)_{qp} := (W_{0h}^p, W_{0h}^q), \quad (\mathbb{B}_0^h)_{qp} := \langle W_{0h}^p, W_{0h}^q \rangle,$$

$$(\mathbb{M}_0^h)_{qp} := (W_{0h}^p, W_{0h}^q),$$

$$(\mathbb{A}_1^h)_{lm} := (W_{1h}^l, W_{1h}^m), \quad (\mathbb{B}_1^h)_{lm} := \langle W_{1h}^l, W_{1h}^m \rangle,$$

$$(\mathcal{C}_1^h)_{lm} := \langle W_{1h}^l, W_{1h}^m \rangle \quad (\mathbf{I})_m := (1, \ 0, \ 0, \cdots, 0)^{\dagger}.$$

The system of algebraic differential equations (3.14) has been solved by using Newton's method. Implementation of numerical scheme is carried out via a MatLab code. Lagrange elements of linear nature have been used to obtain matrices in system (3.14). Simulations of velocity, temperature and concentration for numerous physical parameters have been examined in next section.

4. Simulated results

Simulated results for the velocity, temperature and concentration are discussed in this section. Mainly we focus on the influence of fractional time derivative on the convective transport phenomena using Buongiorno model. Physics of the problem is understood by the variations of non-dimensional parameters. Flow generation, heat and mass transfers are analyzed for the governing mathematical model. Numerical results are noted for the time intervals [0, 2] and [0, $\sqrt{2}$]. Figure 2 is plotted to observe velocity characteristics for numerous values of fractional number α. It is noted by increase of α, velocity increases 2(a). Variations in velocity profile with increase of Hartmann number *Ha* and viscoelastic parameter γ are sketched in figure 2(b). It is noted that velocity decreases with increase of *Ha* and contradictory trends are observed in case of viscoelastic parameter γ. With the increase of *Ha*, Lorentz force enhances that resist fluid motion. Consequently, velocity decreases as *Ha* increases. Effects of mixed convection parameter λ on velocity are sketched in figure 3. It is seen that velocity profile increases with the increase of mixed convection parameter λ 3(a). Inertial forces are inversely related to λ while direct impact is presented for buoyancy forces. When $\lambda > 0$, transfer of heat is from plates to fluid. As a result, $(\theta_{s_1} - \theta_0)$ and $(\theta_{s_2} - \theta_0)$ increase. Consequently, increase in λ, enhances buoyancy forces, $(\theta_{s_1} - \theta_0)$ and $(\theta_{s_2} - \theta_0)$. As a result, fluid velocity increases. Analogous argument can be build for the behavior of nonlinear convection parameter λ_1 3(b). As there is convection, only the mode of convection is nonlinear so as expected results remain same as that of mixed convection parameter λ. Figure 4 is sketched to examine the temperature profile for numerous values of fractional number α. Temperature increases with the increase of α 4(a). Changes in temperature profile with the increase of pedesis parameter *Nb* and Schmidt number *Sc* are sketched in figure 4(b). It is concluded that temperature increases with increase of *Sc* and *Nb*. Momentum diffusivity increases with increase of *Sc* which enhances the friction between different layers of the fluid. Therefore temperature increases with increase of *Sc*. Existence of Brownian coefficient, in the non-dimensional form of *Nb* and decrease of base fluid heat capacity with increase of *Nb*, results in the decrease of temperature. Characteristics of Prandtl number *Pr*, thermophoresis number *Nt* on temperature profile is explored in figure 5. Temperature increases with increase of *Nt* while opposite behavior is noted for *Pr* 5(a). As *Nt* increases, heat capacity of fluid decreases consequently temperature increases with the increase of *Nt*. Thermal diffusivity, decreases with increase of *Pr* consequently temperature remain at lower level for higher value of *Pr*. Figure 5(b) is outlined the effect of heat flux δ and mass flux δ_1 parameters on the temperature. It is concluded that temperature increases with increase of δ while contrary trends are observed for δ_1. Thermal conductivity, of base fluid decreases with the increase of δ which reduces the rate at which the heat passes through the base fluid thus temperature increases with the increase of δ. Figure 6 is plotted to see the change in concentration for numerous values of fractional number α. Concentration increases with the increase of α 6(a). Combined effects of thermophoresis *Nt* and pedesis *Nb* parameters on the concentration are displayed in figure 6(b). Concentration increases with increase of *Nt* while reverse effect is seen for the case of *Nb*. Increase of concentration is due to increase of coefficient of thermophoretic diffusion, present in non-dimensional form of *Nt*. Collective effects of Prandtl *Pr* and Schmidt *Sc* numbers on the concentration profile can be visualized through figure 7. Concentration increases with the increase of *Pr* while opposite trends are seen for *Sc* 7(a). Momentum diffusivity increases with the increase of *Pr*, hence concentration is at higher level for larger value of *Pr*. Fluid viscosity increases while coefficient of Brownian diffusion decreases with increase of *Sc*. Hence concentration profile remains at lower level with the increase of *Sc*. Figure 7(b) is plotted to see the influence of heat flux δ and mass flux δ_1 parameters on the concentration. Concentration increases with increase of δ and δ_1. Rate of concentration transfer decreases with increase of δ_1 thus concentration increases with increasing values of δ_1. Finally figures 8(a), (b), 9(a), (b) are sketched for time dependent

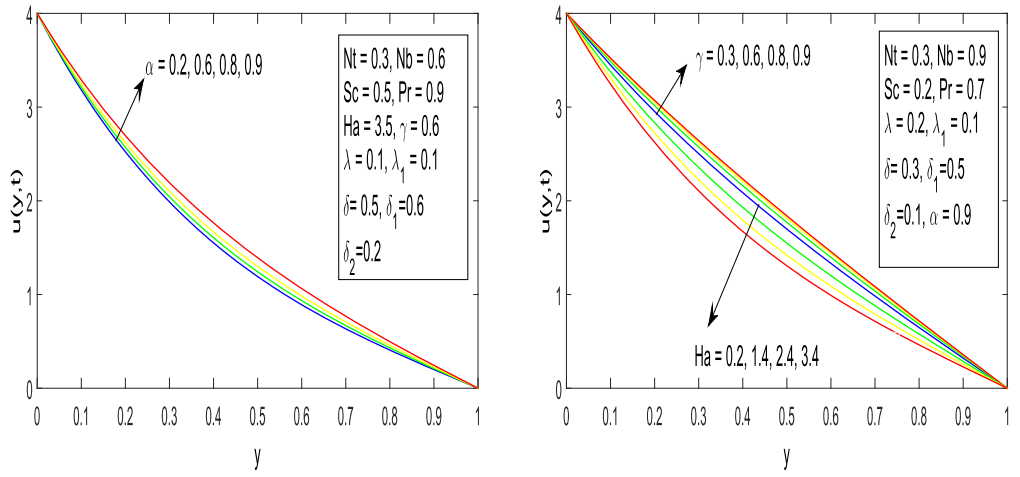

(a) Variations of velocity profile with α. (b) Variations of velocity profile with Ha and γ.

Figure 2. Effects of non-integer exponent, Hartmann number and viscoelastic parameter on the velocity profile.

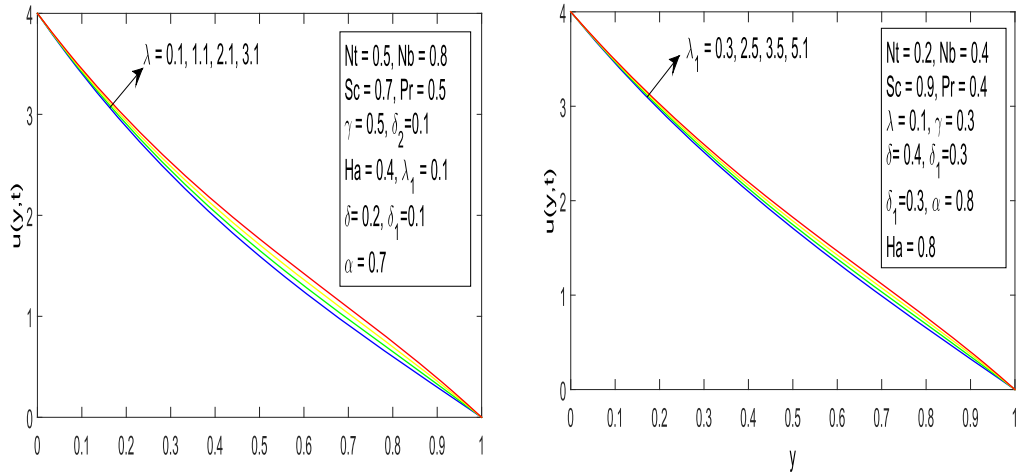

(a) Variations of velocity profile with λ. (b) Variations of velocity profile with λ_1.

Figure 3. Effects convection parameters on the velocity profile.

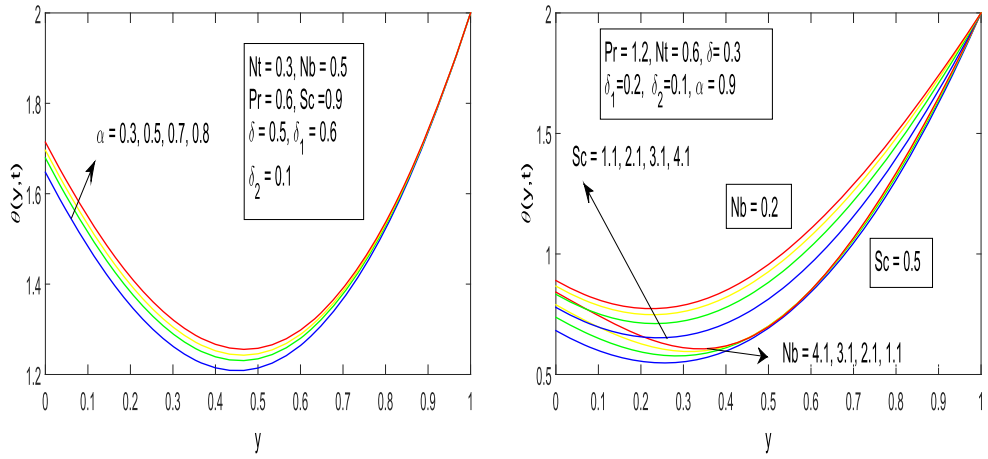

(a) Variations of temperature profile with α. (b) Variations of temperature profile with Sc and Nb.

Figure 4. Effects of non-integer exponent, pedesis parameter and Schmidt number on the temperature profile.

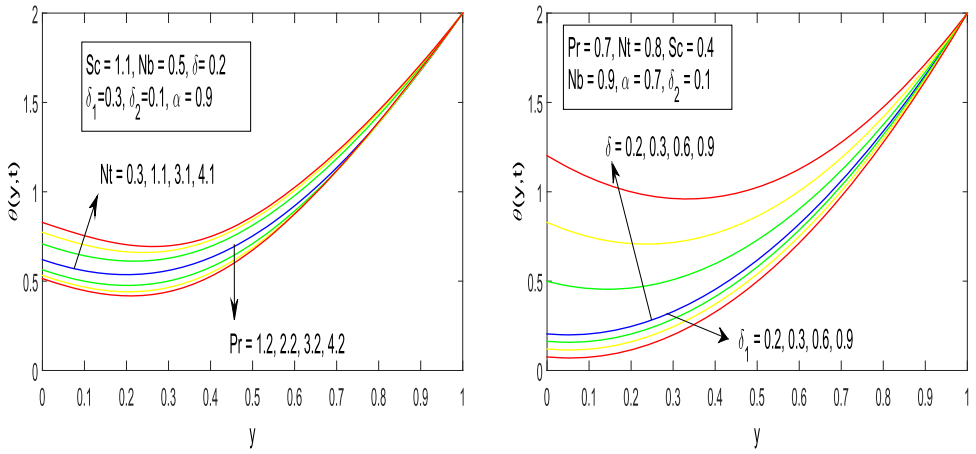

(a) Variations of temperature profile with Pr and Nt.(b) Variations of temperature profile with δ and δ_1.

Figure 5. Effects of Prandtl number, thermophoresis, heat and mass flux parameters on temperature profile.

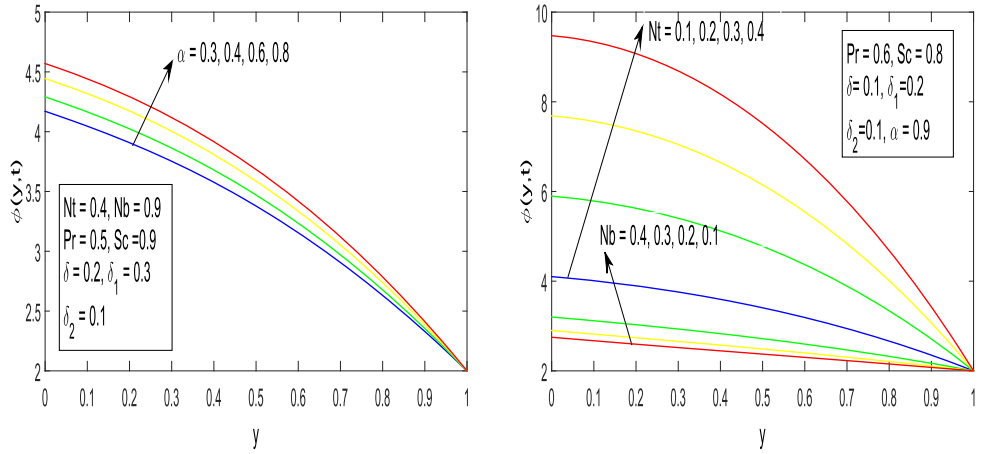

(a) Variations of concentration profile with α. (b) Variations of concentration profile with Nt and Nb.

Figure 6. Effects of non-integer exponent, thermophoresis and pedesis parameters on the concentration profile.

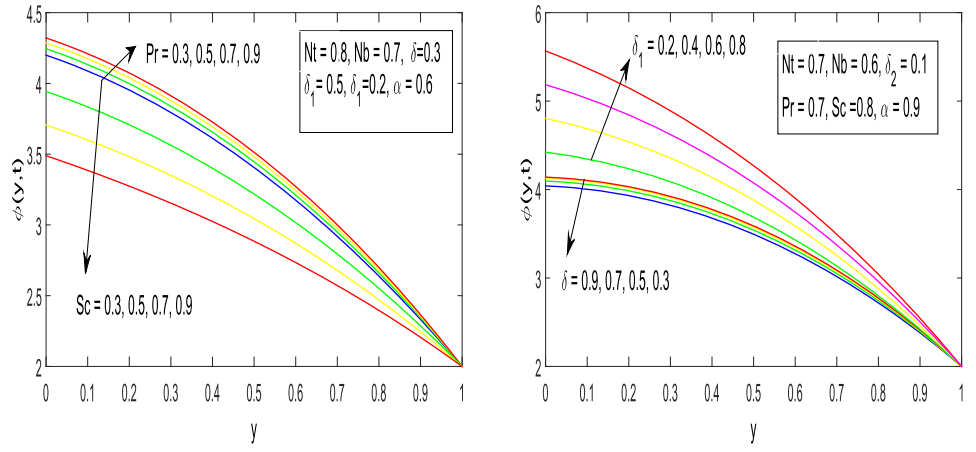

(a) Variations of concentration profile with Pr and Sc.(b) Variations of concentration profile withδ and δ_1.

Figure 7. Effects of Prandtl number, Schmidt number, heat flux and mass flux parameters on the concentration profile.

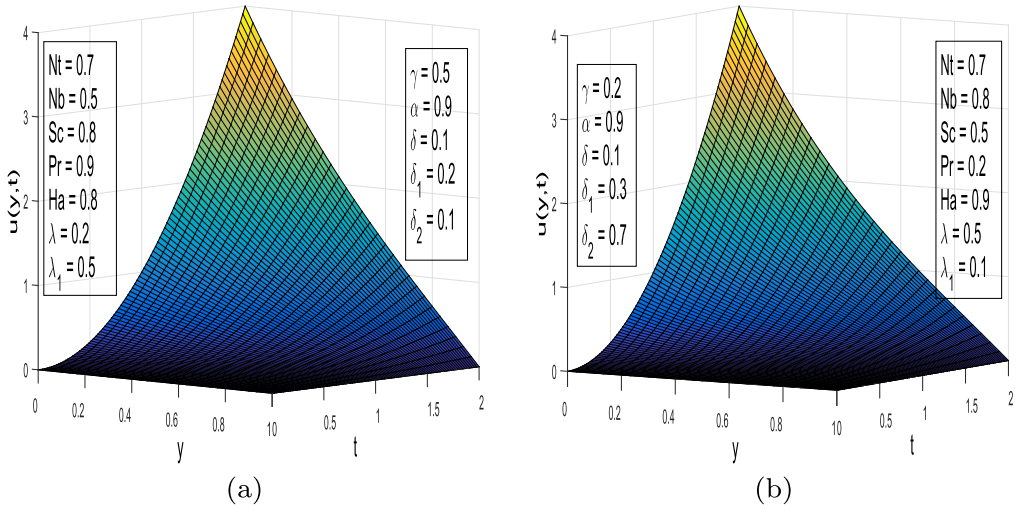

Figure 8. Transient velocity profiles for different values of parameters over the time interval [0, 2].

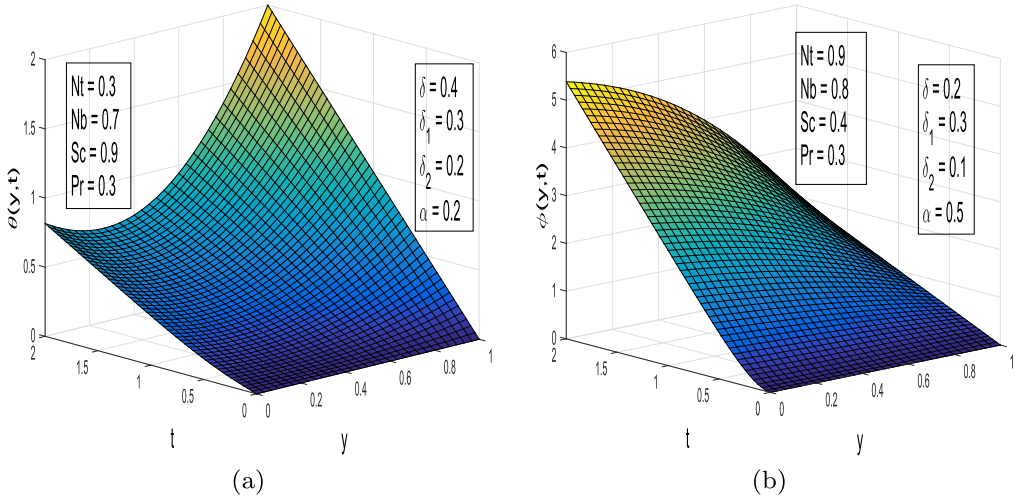

Figure 9. Transient temperature and concentration profiles for different values of parameters over the time interval [0, $\sqrt{2}$].

velocity, temperature and concentration profiles. These figures demonstrated anomalous behavior of fractional nanofluid. Variations of skin friction and Nusselt numbers with pertinent fractional model parameters are examined via tables 1–3. Skin friction magnitude, increases with increase of α, δ_2, *Pr* and *Ha* while it decreases with increase of γ, λ, λ_1, δ, *Sc*, *Nt* and *Nb*. Moreover Nusselt number at the lower plate increases with the increase of *Pr* while it decreases with the increase of *Nt*, *Nb* and δ_2.

5. Conclusion

Fractional formalism of the Buongiorno model with Caputo derivative is constructed in this study. Viscous as well as elastic characteristics of the viscoelastic fluid is observed via non-integer time derivatives. Fractional relaxation times are introduced to control the transport process. In order to deeply observe the influence of buoyancy forces on the flow regime, nonlinear convection is introduced in the mathematical modeling of the flow problem. Brownian motion and thermophoresis effects are also tackled in a nanofluid flow. Flow behavior is handled by the applied magnetic field. Change in temperature and concentration with respect to their gradients is noted at the lower boundary. Numerical technique, which includes finite element discretization for the space variable while finite difference discretization of the Caputo fractional derivative, is applied to solve the governing highly nonlinear flow differential equations. Fractional time derivative α tends to increase the velocity, temperature and concentration profiles. Consequently, parameter α helps to control the transport process in the flow domain. The abrupt changes in heat and mass transfer which may be seen in Buongiorno model, can be easily handled with α. Brownian motion and thermophoresis parameters have similar effects on the temperature profile while opposite behavior is noted in the case of concentration profile. Applications of these flows can be seen in geology and fiber technology. The study can be extended for relaxation time phenomena in Maxwell fluid flow. An

Table 1. Effects of non linear flow model parameters on the skin friction coefficient at $(y, t) = (0, 0.1)$ when $Nt = 0.4$, $Nb = 0.3$, $Sc = 0.8$, $Pr = 0.7$, $\delta = 0.5$, $\delta_1 = 0.8$, $\delta_2 = 0.02$ and $\alpha = 0.4$.

γ	λ	λ_1	Ha	$ReC_f/2$
0.2	0.3	0.1	0.4	−2.772 31
0.3				−2.507 821
0.4	0.3			−2.312 489
	0.4			−2.177 760
	0.5	0.1		−2.156 345
		0.2		−2.153 404
		0.3	0.4	−2.151 162
			0.5	−2.178 998
			0.6	−2.198 633

Table 2. Effects of non linear flow model parameters on the skin friction coefficient at $(y, t) = (0, 0.1)$ when $\gamma = 0.6$, $Ha = 0.6$, $\delta_1 = 0.02$, $\lambda = 0.6$ and $\lambda_1 = 0.5$.

α	δ	δ_1	Pr	Sc	Nt	Nb	$ReC_f/2$
0.3	0.6	0.6	0.4	0.7	0.5	0.6	−0.325 326
0.4							−0.586 382
0.5	0.6						−0.956 314
	0.7						−0.880 353
	0.8	0.6					−0.856 701
		0.7					−0.834 365
		0.8	0.4				−0.832 710
			0.5				−0.880 274
			0.6	0.7			−0.912 904
				0.8			−0.912 844
				0.9	0.5		−0.912 748
					0.6		−0.912 462
					0.7	0.6	−0.912 184
						0.7	−0.911 957
						0.8	−0.911 695

Table 3. Effects of non linear flow model parameters on the Nusselt numbers at $t = 0.1$ when $\alpha = 0.4$, $\delta = 0.1$, $Sc = 0.4$, and $\delta_1 = 0.2$.

Pr	Nt	Nb	δ_2	Nu_1/Re	Nu_2/Re^2
0.2	0.1	0.2	0.3	0.652 761	0.977 892
0.3				0.632 321	0.998 214
0.4	0.1			0.612 524	1.542 145
	0.2			0.622 487	1.532 148
	0.3	0.2		0.645 121	1.512 144
		0.3		0.652 489	1.502 354
		0.4	0.3	0.665 297	1.493 233
			0.4	0.632 145	1.482 564
			0.5	0.612 547	1.475 867

investigation can also be considered to handle nonlinear radiation aspects in a nanofluid with fractional derivative.

Competing interest

The Author, affirm that he has no competing interests.

ORCID iDs

Muhammad Shoaib Anwar https://orcid.org/0000-0001-5141-9838

References

[1] Akbar N S, Tripathi D and Khan Z H 2018 Numerical investigation of Cattanneo–Christov heat flux in CNT suspended nanofluid flow over a stretching porous surface with suction and injection *Discrete Continuous Dyn. Syst.* S **11** 595–606

[2] Aziz A and Jamshed W 2018 Unsteady MHD slip flow of non Newtonian power-law nanofluid over a moving surface with temperature dependent thermal conductivity *Discrete Continuous Dyn. Syst.* S **11** 617–30

[3] Kirby B J 2010 *Micro and Nanoscale Fluid Mechanics: Transport in Microfluidic Devices* (Cambridge: Cambridge University Press)

[4] Sheikholeslami M and Ganji D D 2015 Nanofluid flow and heat transfer between parallel plates considering Brownian motion using DTM *Comput. Methods Appl. Mech. Eng.* **283** 651–63

[5] Liu Y and He J-H 2011 Bubble electrospinning for mass production of nanofibers *Int. J. Nonlinear Sci. Numer. Simul.* **8** 393–6

[6] Valipour P, Zaersabet H, Hatami M, Zolfagharian A and Ghasemi S E 2017 Numerical study on polymer nanofibers with electrically charged jet of viscoelastic fluid in electrospinning process *J. Cent. South Univ.* **24** 2275–80

[7] Wang G and Zhang J 2017 Thermal and power performance analysis for heat transfer applications of nanofluids in flows around cylinder *Appl. Ther. Eng.* **112** 61–72

[8] Buongiorno J 2006 Convective transport in nanofluids *ASME, J. Heat Transfer* **128** 240–50

[9] Podlubny I 1999 *Fractional Differential Equations* (New York: Academic)

[10] Sabatier J, Agrawal O P and Tenreiro Machado J A 2007 *Advances in Fractional Calculus: Theoretical Developments and Applications in Physics and Engineering* (Netherlands: Springer, Dordrecht)

[11] Ahokposi D P, Atangana A and Vermeulen D P 2017 Modelling groundwater fractal flow with fractional differentiation via Mittag–Leffler law *Eur. Phys. J. Plus* **132** 165

[12] Atangana A and Baleanu D 2016 New fractional derivatives with non-local non-singular kernel: theory and application to heat transfer model *Therm. Sci.* **20** 763–9

[13] Sheikh N A, Ali F, Saqib M, Khan I, Alam Jan S A, Alshomrani A S and Alghamdi M S 2017 Comparison and analysis of the Atangana–Baleanu and Caputo–Fabrizio fractional derivatives for generalized Casson fluid model with heat generation and chemical reaction *Results Phys.* **7** 789–800

[14] Ali F, Sheikh N A, Khan I and Saqib M 2017 Magneticfield effect on bloodflow of Cassonfluid in axisymmetric cylindrical tube: a fractional model *J. Magn. Magn. Mater.* **423** 327–36

[15] Sheikh N A, Ali F, Saqib M, Khan I and Alam Jan S A 2017 A comparative study of Atangana–Baleanu and Caputo–Fabrizio fractional derivatives to the convective flow of a generalized Casson fluid *Eur. Phys. J. Plus* **132** 54

[16] Khan M, Ali S H and Qi H 2009 On accelerated flows of a viscoelastic fluid with the fractional Burgers' model *Nonlinear Anal. Real World Appl.* **10** 2286–96

[17] Zhao J, Zheng L, Zhang X and Liu F 2016 Unsteady natural convection boundary layer heat transfer of fractional Maxwell viscoelastic fluid over a vertical plate *Int. J. Heat Mass Transfer* **97** 760–6

[18] Yang Xiao-Jun 2017 General fractional calculus operators containing the generalized Mittag–Leffler functions applied to anomalous relaxation *Therm. Sci.* **21** S317–26
[19] Makris N, Dargush G F and Constantinou M C 1993 Dynamic analysis of generalized viscoelastic fluids *J. Eng. Mech.* **119** 1663–79
[20] Anwar M S and Rasheed A 2017 Simulations of a fractional rate type nanofluid flow with non-integer Caputo time derivatives *Comput. Math. Appl.* **74** 2485–502
[21] Zhou Z and Liang D 2017 The mass-preserving and modified-upwind splitting DDM scheme for time-dependent convection–diffusion equations *J. Comput. Appl. Math.* **317** 247–73
[22] Julyan J and Hutchinson A J 2018 Conservation laws and conserved quantities of the governing equations for the laminar wake flow behind a small hump on a solid wall boundary *Int. J. Non-Linear Mech.* **100** 48–57
[23] Salama A, Sun S and Wheeler M F 2014 Solving global problem by considering multitude of local problems: application to fluid flow in anisotropic porous media using the multipoint flux approximation *J. Comput. Appl. Math.* **267** 117–30
[24] Rasheed A and Anwar M S 2018 Simulations of variable concentration aspects in a fractional nonlinear viscoelastic fluid flow *Commun. Nonlinear Sci. Numer. Simul.* **65** 216–30
[25] Waqas M, Ijaz Khan M, Hayat T and Alsaedi A 2017 Numerical simulation for magneto Carreau nanofluid model with thermal radiation: a revised model *Comput. Methods Appl. Mech. Eng.* **324** 640–53
[26] Lin Y and Xu C 2007 Finite difference/spectral approximations for the time-fractional diffusion equation *J. Comput. Phys.* **225** 1533–52
[27] Abd El-Lateif A M and Abdel-Hameid A M 2017 Comment on 'Solutions with special functions for time fractional free convection flow of Brinkman-type fluid' by F Ali *et al Eur. Phys. J. Plus* **132** 407
[28] Adams R A 1975 *Sobolev Spaces* (New York: Academic)